

Microfluidic Particle Dam for Visual and Quantitative Detection of Lead Ions

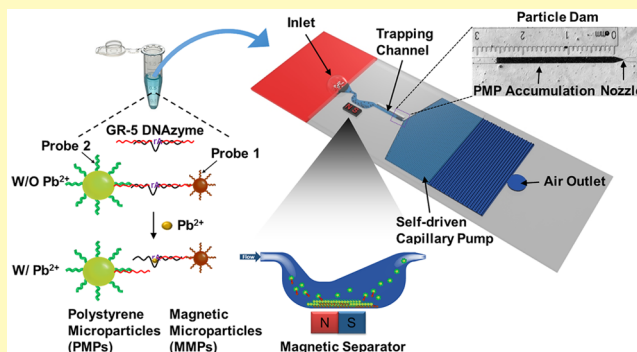
Gaobo Wang,^{†,#} Lok Ting Chu,^{†,#} Hogi Hartanto,[†] William Budi Utomo,[†] Reynard Aaron Pravasta,[‡] and Ting-Hsuan Chen^{*,†}

[†]Department of Biomedical Engineering and [‡]Department of Mechanical Engineering, City University of Hong Kong, Hong Kong, Hong Kong Special Administrative Region

Supporting Information

ABSTRACT: Lead contamination in drinking water is a primary concern in public health, but it is difficult to monitor by end-users. Here, we provide a rapid and power-free microfluidic particle dam which enables visual quantification of lead ions (Pb^{2+}) by the naked eye. GR-5 DNAzyme with extended termini can connect magnetic microparticles (MMPs) and polystyrene microparticles (PMPs) by DNA hybridization, forming “MMPs-GR-5-PMPs”. When Pb^{2+} is present, GR-5 is cleaved, resulting in an increasing number of free PMPs. To visually count the free PMPs, the solution is loaded to a capillary-driven microfluidic device that consists of a magnetic separator to remove the MMPs-GR-5-PMPs, followed by a particle dam that traps and accumulates the free PMPs into a visual bar with growing length proportional to the concentration of lead. The device achieved a limit of detection at 2.12 nM (0.44 ppb), high selectivity (>20,000-fold) against other metal ions, high tolerance to different pH and water hardness, and is compatible with tap water with a high recovery rate, enabling visual quantification and user-friendly interface for rapid screening of water safety.

KEYWORDS: particles, lead, DNAzyme, microfluidics, visual detection



Lead ions (Pb^{2+}) have been a severe threat to the environment and public health. It is especially a primary concern in drinking water since lead can accumulate in organs or tissues after chronic exposure, resulting in neurological, reproductive, cardiovascular, and developmental disorders.¹ To determine the lead ions, standard platforms, including atomic absorption spectrometry, inductively coupled plasma, atomic emission spectrometry, and mass spectrometry have been widely used.^{2–4} However, it requires expensive equipment, sophisticated sample preparation, and skilled operators, making the detection procedures time-consuming and not accessible by ordinary end-users.

Therefore, considerable efforts have been spent to develop miniaturized analytical tools for simple and sensitive detection of lead ions. In the past decades, functional nucleic acids (FNAs) have exhibited their great potential in the field of analytical applications.^{5–7} Artificial FNAs, including ribozymes, deoxyribozymes (DNAzymes), and aptamers, are of great importance for quantitative detection of lead ions due to the advantages of low cost, high affinity, high sensitivity, and excellent stability.^{1,8–12} GR-5 DNAzyme is a commonly used FNA that exhibits highly sensitive and selective hydrolytic cleavage with the presence of lead ions.^{13,14} Wang et al. developed a fluorescence biosensor based on GR-5 DNAzyme modified on gold nanoparticles (AuNPs). With the presence of

lead ions, the GR-5 DNAzyme is cleaved, resulting in a fluorescence signal due to the releasing of a short FAM-linked oligo fragment.¹⁰ Meanwhile, the cleavage of DNAzyme can also induce different aggregation states of gold nanoparticles, inducing a color change observed by visual inspection.¹⁵ To further simplify and miniaturize the lead detection, DNAzyme has been used in microfluidics systems with reporters such as fluorescent tag,¹⁶ electrochemiluminescence,¹⁷ glucose,^{18,19} or redox-active ferrocene for electrochemical signal.²⁰ To provide visual signals, the presence of lead ions can also lead to formation of a visible bar by deposition of gold nanoparticles in a lateral flow dipstick,²¹ aggregation of gold nanoparticles along with the laminar flow in the microchannels,²² or movement of an ink bar in volumetric bar-chart chip.²³ Alternatively, other detection strategies such as combining the graphene oxide quantum dot with fluorescence quenching methods²⁴ and lead specific fluorescent molecular sensor CalixDANS4²⁵ were also proposed.

Although many detection strategies were developed, quantitative analysis has been challenging. Generally, fluorescence, colorimetric, or visual detection requires special

Received: October 2, 2019

Accepted: December 6, 2019

Published: December 6, 2019

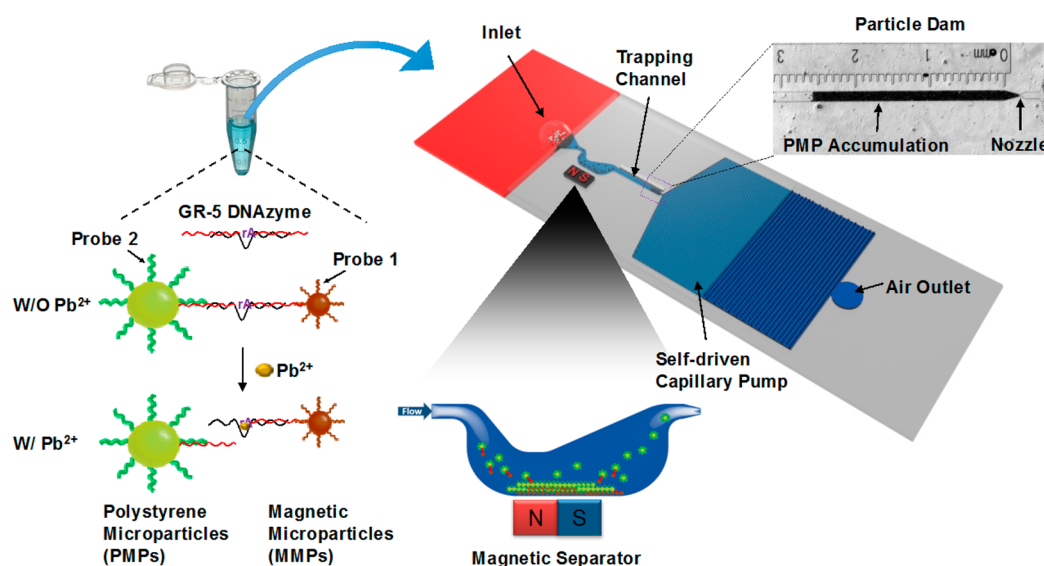


Figure 1. Schematic illustration of the working principle. The lead ions can cleave the GR-5 DNAzyme, preventing the connection between magnetic microparticles (MMPs) and polystyrene microparticles (PMPs). After loading to a capillary microfluidic device, the free PMPs can first pass the magnetic separator, which removes the MMPs-GR-5-PMPs, and continue to flow until being trapped by the particle dam with a nozzle, forming a visual bar by PMP accumulation reflecting the concentration of lead ions.

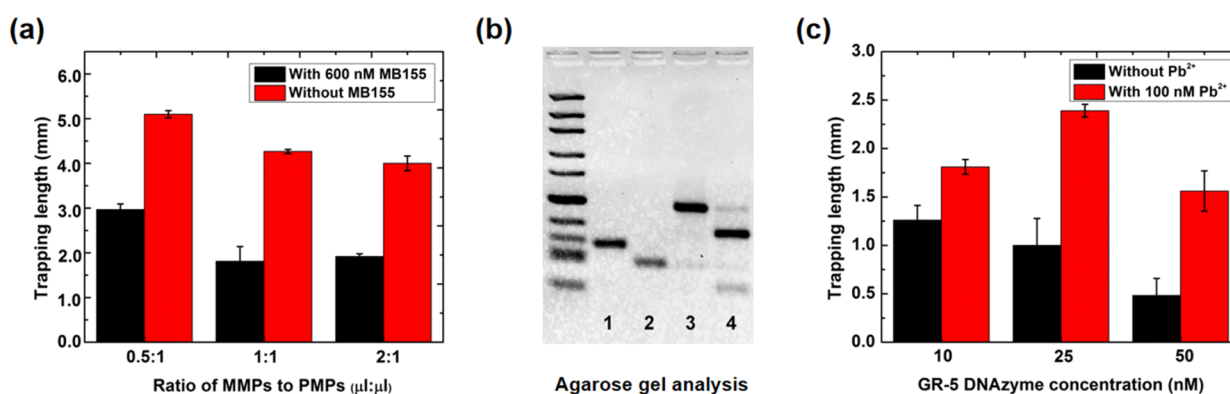


Figure 2. Optimization of lead detection. (a) Optimization of the ratio of MMPs to PMPs using MB155 as a single strand oligonucleotide to connect MMPs and PMPs. (b) Agarose gel analysis. Well 1: GRDS (Substrate strand); Well 2: GRE (Enzyme strand); Well 3: GR-5 DNAzyme; Well 4: GR-5 DNAzyme + Pb²⁺ (200 nM). (c) Optimization of GR-5 concentration.

fluorescence/optical detector or a standard color table, making the results ambiguous and difficult to interpret. It is even more complicated to install benchtop instrumentation on a miniaturized device for quantitative analysis. On the other hand, electrochemistry-based measurement and volumetric bar-chart chip are effective approaches to quantitatively determine trace lead ions.^{20,23} However, delicate operation and nontrivial protocol are required for preparing such reactions, creating technical hurdles for on-site and real-time detection by untrained end-users.

Here, we provide a simple and sensitive microfluidic particle dam which enables visual quantification of lead ions (Pb²⁺) by the naked eye. GR-5 DNAzyme with extended termini is utilized to hybridize with the oligonucleotides on magnetic microparticles (MMPs) and polystyrene microparticles (PMPs), forming “MMPs-GR-5-PMPs”. Importantly, the GR-5 is cleaved when Pb²⁺ is present, resulting in an increasing number of free PMPs proportional to the amount of lead ions. To quantify it, an automated, capillary-driven microfluidic device consisting of a magnetic separator is used to remove the MMPs-GR-5-PMPs, leaving the free PMPs continuing to flow

until being trapped by a particle dam in downstream. Thus, the PMP accumulation eventually forms a visual bar quantifiable by the length (Figure 1). We first optimized the experimental conditions including particle ratio and GR-5 concentration. Next, to test its function, we explored the limit of detection, tolerance to different pH and water hardness, and selectivity against other metal ions. Finally, we explored the feasibility of application in tap water.

RESULTS AND DISCUSSION

Working Principle of the Microfluidic Device. The device consists of an inlet for sample loading. We intentionally make the outer region of the inlet hydrophobic, which is opposed to the hydrophilic inner walls of the microchannel. Thus, when the particle solution is deposited at the inlet, the wettability contrast ensures all particle solution is pumped into the microchannel (Figure S1). After loading, the self-driven capillary flow carries the solution to first pass a stomach-shaped magnetic separator for separating free PMPs from the MMPs-GR-5-PMPs. For the blank control, most of MMPs-GR-5-PMPs are attracted by the permanent magnets in the

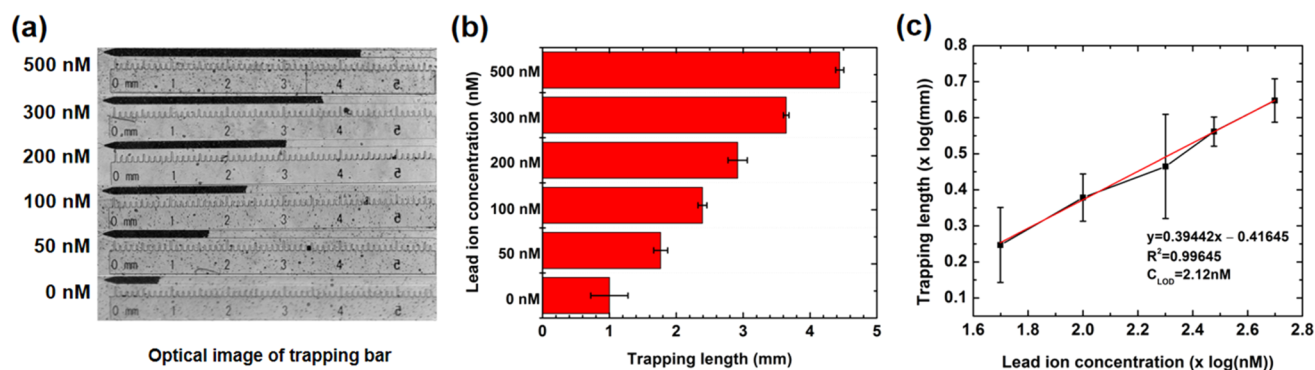


Figure 3. Limit of detection. (a) Optical images of the PMP accumulation resulted from various lead ion concentrations. (b) Length of accumulated PMPs in the trapping channel (mean \pm max deviation, $n = 3$). (c) Linear regression of the trapping length with respect to each concentration of lead ions (mean \pm max deviation, $n = 3$).

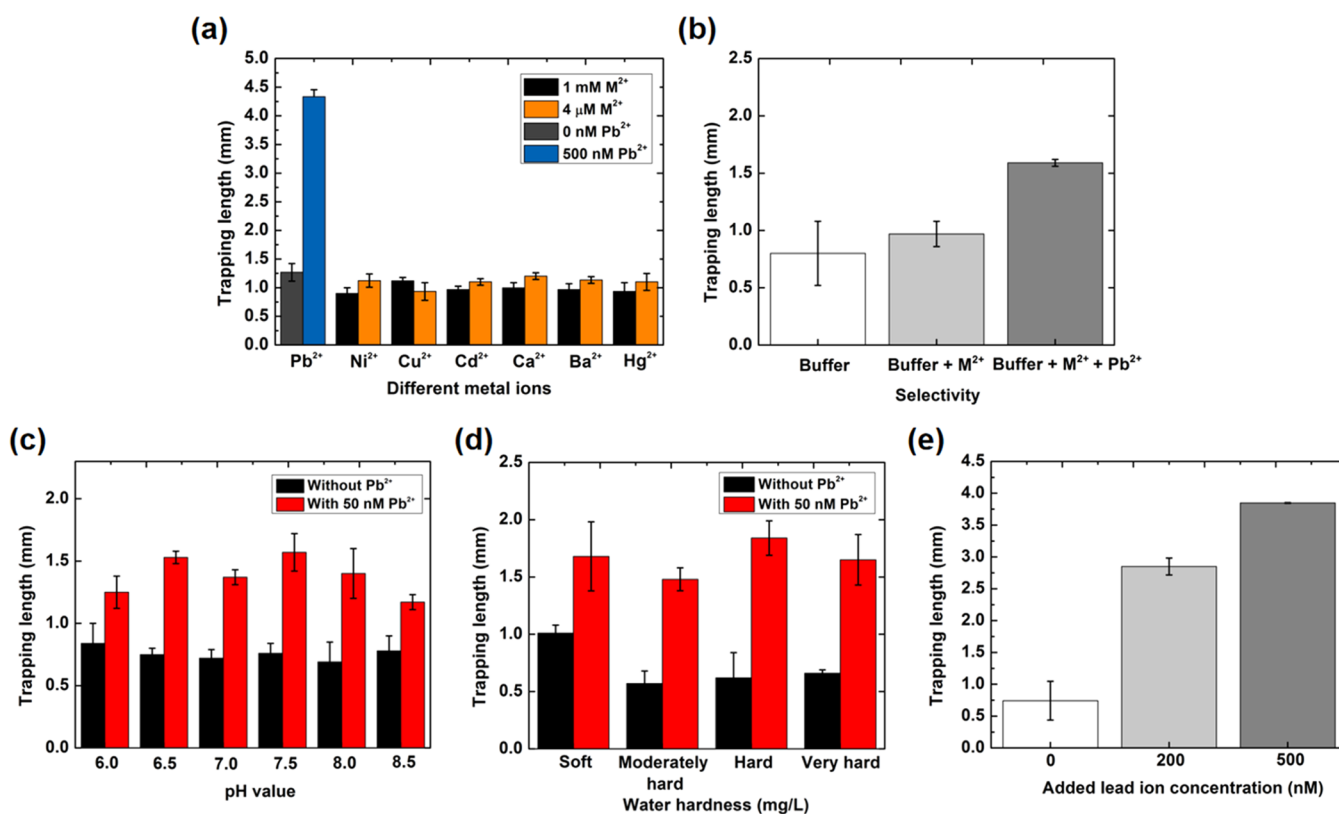


Figure 4. Practicality of the lead detection. (a) Selective detection of lead ions (500 nM) against other metal ions with higher concentration (4 μM/1 mM) (mean \pm max deviation, $n = 3$). (b) Selective detection of lead ion in the presence of other metal ions (Buffer: blank buffer sample without addition of metal ions; M²⁺: addition of all metal ions other than Pb²⁺ in 1 mM; Pb²⁺: addition of Pb²⁺ in 50 nM). (c) Lead detection in different pH conditions. (d) Lead ion detection in different water hardness levels. Soft: 55 mg/L; Moderately Hard: 107.5 mg/L; Hard: 157.7 mg/L; Very Hard: 318.3 mg/L. (e) Detection in tap water with spiked lead ions.

bottom of the magnetic separator (Video S1). When lead is present (200 nM), the free PMPs can pass the magnetic field (Video S2) and continue to flow until being stopped at a particle dam with a nozzle (narrowest width = 8 μm), which can trap and accumulate PMPs with diameter of 15.34 μm in the trapping channel (Video S3). Thus, the amount of free PMPs can be read and visually quantified by the trapping length.

Optimization of Experimental Conditions. We first optimized the ratio of MMPs and PMPs to maximize the signal-to-noise ratio. A mixture of disconnected MMPs and PMPs was used to represent the broken GR-5 connection after

hydrolytic cleavage by lead ions. For simplicity, single strand oligonucleotide MB155 with sequence complementary to Probe 1 and Probe 2 in juxtaposition (600 nM in 1 μL, sequence in Table S1), was used to connect the MMPs and PMPs, forming MMPs-MB155-PMPs representing the MMPs-GR-5-PMPs. As opposed to blank control without MB155, we used a relatively higher concentration of MB155 to ensure that all MMPs and PMPs can be linked. We found that the ratio of MMPs to PMPs at 1:1 (volume ratio of the stock solution) provided the optimal relative contrast (Figure 2a), as magnetic attraction was insufficient at the ratio of 0.5:1, and no

improvement was gained when MMPs were increased to 2:1 ratio. Thus, 1:1 ratio of MMPs and PMPs was used in follows.

We next optimized the concentration of GR-5 used to connect microparticles for lead detection. As shown in the gel electrophoresis result (Figure 2b), GR-5 was formed by hybridization between substrate strand GRDS and enzyme strand GRE at 1:1 ratio, but was cleaved at RNA site (rA) of substrate strand with the presence of lead ions, which would result in the disconnection between MMPs and PMPs. By testing different GR-5 concentrations (Figure 2c), we found that the optimal concentration of GR-5 DNAzyme is 25 nM since less GR-5 DNAzyme (10 nM) would cause the insufficient linkage between MMPs and PMPs, while too concentrated GR-5 DNAzyme (50 nM) would induce low sensitivity because it requires more lead ions to cleave the GR-5.

Limit of Detection. Based on the optimized particle ratio (1:1) and the GR-5 concentration (25 nM) (Figure 2), we next explored the limit of detection by a set of lead ion solution with various concentrations (0 nM, 50 nM, 100 nM, 200 nM, 300 nM, and 500 nM). As expected, increasing lead concentration led to an increase of PMP accumulation length, which can be observed and quantified by the naked eye (Figure 3a). Based on the measured trapping length (Figure 3b) and the lineage regression (Figure 3c), a limit of detection of 2.12 nM (0.44 ppb) was determined ($S/N = 3$, calculated on the basis of $3\sigma/k$, where σ is the standard deviation of the blank control, and k is the absolute slope of the linear equation, 0.39442), which is around 35 times below the required 15 ppb of permissible concentration defined by the U.S. Environmental Protection Agency.

Selectivity. To investigate the selectivity of our device, different metal ions such as Nickel (Ni^{2+}), Copper (Cu^{2+}), Cadmium (Cd^{2+}), Calcium (Ca^{2+}), Barium (Ba^{2+}), and Mercury (Hg^{2+}) were used. With 500 nM of lead ions, the trapping length can reach up to 4.5 mm, which means that GR-5 DNAzyme was cleaved in the presence of lead ions (Figure 4a). In contrast, for other metal ions with much higher concentration (4 μM and 1 mM), the trapping length was similar to that of the blank control without metal ions, indicating that other metal ions cannot cleave the GR-5 DNAzyme. Moreover, to investigate the possible interference on lead detection when other metal ions are simultaneously present, we detect Pb^{2+} (50 nM) in a mixture of all other metal ions (Nickel (Ni^{2+}), Copper (Cu^{2+}), Cadmium (Cd^{2+}), Calcium (Ca^{2+}), Barium (Ba^{2+}), and Mercury (Hg^{2+})) with much higher concentration (1 mM). The results showed that our detection is not interfered by other metal ions (Figure 4b). After calculation, the selectivity achieved >20,000-fold.

Tolerance to Acidity/Basicity. To investigate the tolerance to water source with different acidity/basicity, lead ions were spiked in water with adjusted pH = 6.0–8.5, which represents the acidic/basic condition in the groundwater system (pH = 6.0–8.5) and the surface water systems (pH = 6.5–8.5). The results showed clear difference in trapping length between samples with and without 50 nM lead ions, suggesting the suitability of detection in ground and surface water systems. For pH 6.0 and 8.5, the difference of trapping length was slightly reduced (Figure 4c), which might be because the GR-5 DNAzyme becomes unstable and even causes nonspecific binding between microparticles when the pH value is beyond the range of 6.5–8.0.

Tolerance to Water Hardness. To test the tolerance to water hardness, we adopted four kinds of water samples with different hardness levels (Soft (55 mg/L), Moderately Hard (107.5 mg/L), Hard (157.7 mg/L), and Very Hard (318.3 mg/L) according to the water hardness scale from World Health Organization). The results showed clear and consistent distinction in trapping length between samples with and without 50 nM lead ion, suggesting high tolerance to water hardness (Figure 4d).

Detection in Tap Water. To demonstrate the practical application of our method, we challenged our microchip for the detection of lead ions in tap water. Original lead ions concentration in tap water was determined as 8.68 nM by ICP-MS. In our device, the trapping length resulting from tap water was 0.74 ± 0.3 mm. According to the linear regression as a calibration line (Figure 3c), the lead concentration can be calculated as 6.48 ± 4.92 nM, which is 74.7% recovery as compared to the original lead concentration 8.68 nM (Figure 4e and Table 1). In addition, with spiked lead at concentration

Table 1. Detection in Tap Water with Spiked Lead Ions

sample	original (nM)	added (nM)	found (nM) [mean \pm SD]	recovery (%)
Tap water 1	8.68	0	6.48 ± 4.92	74.7
Tap water 2	8.68	200	162.3 ± 19.4	77.8
Tap water 3	8.68	500	346.15 ± 1.316	68.1

of 200 nM and 500 nM, high recovery rates were again observed at 77.8% and 68.1%, respectively, which exhibits good practicability for the lead ion detection in real water samples.

CONCLUSIONS

Lead contamination in drinking water has become a global concern in public health. A simple, user-friendly, and inexpensive detection strategy is highly desired. Here, based on accumulation of PMPs at the particle dam, we demonstrate a rapid and self-driven microchip enabling visual quantification of lead ions (Pb^{2+}) by the naked eye. We achieved a limit of detection at 2.12 nM (0.44 ppb), which is 35 times below the required 15 ppb of permissible concentration defined by U.S. Environmental Protection Agency. Also, high selectivity (>20,000-fold) against other metal ions, high tolerance to different pH and water hardness, and compatibility with tap water with high recovery rate were also demonstrated. Together, this portable, power-free, label-free, and low cost microfluidic strip allows simple and rapid screening for end users to monitor water safety.

ASSOCIATED CONTENT

Supporting Information

The Supporting Information is available free of charge at <https://pubs.acs.org/doi/10.1021/acssensors.9b01945>.

Experimental section; layout of the microfluidic chip; fabrication process; contact angle measurement of different surface-treatment on NOA and glass; sequence of oligonucleotides (PDF)

Magnetic separation without lead ions (MP4)

Magnetic separation with 200 nM of lead ions (MP4)

PMP accumulation at the particle dam (MP4)

AUTHOR INFORMATION

Corresponding Author

*E-mail: thchen@cityu.edu.hk.

ORCID

Ting-Hsuan Chen: 0000-0003-4517-7750

Author Contributions

#Gaobo Wang and Lok Ting Chu contributed equally to this work.

Notes

The authors declare no competing financial interest.

ACKNOWLEDGMENTS

We are pleased to acknowledge the funding support from the Early Career Scheme (project no. 21214815), General Research Fund (project nos. 11277516 and 11217217), and NSFC/RGC Joint Research Scheme (N_CityU119/19) from the Hong Kong Research Grant Council, and internal grants from City University of Hong Kong (9667161 and 6000632).

REFERENCES

- (1) Yang, D.; Liu, X.; Zhou, Y.; Luo, L.; Zhang, J.; Huang, A.; Mao, Q.; Chen, X.; Tang, L. Aptamer-based biosensors for detection of lead(II) ion: a review. *Anal. Methods* **2017**, *9*, 1976–1990.
- (2) Townsend, A. T.; Miller, K. A.; McLean, S.; Aldous, S. The determination of copper, zinc, cadmium and lead in urine by high resolution ICP-MS. *J. Anal. At. Spectrom.* **1998**, *13*, 1213–1219.
- (3) Deng, W.; Hong, L. R.; Zhao, M.; Zhuo, Y.; Gao, M. Electrochemiluminescence-based detection method of lead(II) ion via dual enhancement of intermolecular and intramolecular co-reaction. *Analyst* **2015**, *140*, 4206–4211.
- (4) Khoshbin, Z.; Housaindokht, M. R.; Verdian, A.; Bozorgmehr, M. R. Simultaneous detection and determination of mercury (II) and lead (II) ions through the achievement of novel functional nucleic acid-based biosensors. *Biosens. Bioelectron.* **2018**, *116*, 130–147.
- (5) Hu, R.; Zhang, X.-B.; Kong, R.-M.; Zhao, X.-H.; Jiang, J.; Tan, W. Nucleic acid-functionalized nanomaterials for bioimaging applications. *J. Mater. Chem.* **2011**, *21*, 16323–16334.
- (6) Li, W.; Yang, Y.; Chen, J.; Zhang, Q.; Wang, Y.; Wang, F.; Yu, C. Detection of lead(II) ions with a DNAzyme and isothermal strand displacement signal amplification. *Biosens. Bioelectron.* **2014**, *53*, 245–249.
- (7) Dolati, S.; Ramezani, M.; Abnous, K.; Taghdisi, S. M. Recent nucleic acid based biosensors for Pb²⁺ detection. *Sens. Actuators, B* **2017**, *246*, 864–878.
- (8) Lan, T.; Furuya, K.; Lu, Y. A highly selective lead sensor based on a classic lead DNAzyme. *Chem. Commun. (Cambridge, U. K.)* **2010**, *46*, 3896–3898.
- (9) Wen, Y.; Peng, C.; Li, D.; Zhuo, L.; He, S.; Wang, L.; Huang, Q.; Xu, Q. H.; Fan, C. Metal ion-modulated graphene-DNAzyme interactions: design of a nanoprobe for fluorescent detection of lead(II) ions with high sensitivity, selectivity and tunable dynamic range. *Chem. Commun. (Cambridge, U. K.)* **2011**, *47*, 6278–6280.
- (10) Wang, H.-B.; Wang, L.; Huang, K.-J.; Xu, S.-P.; Wang, H.-Q.; Wang, L.-L.; Liu, Y.-M. A highly sensitive and selective biosensing strategy for the detection of Pb²⁺ ions based on GR-5 DNAzyme functionalized AuNPs. *New J. Chem.* **2013**, *37*, 2557–2563.
- (11) Sharma, R.; Ragavan, K. V.; Thakur, M. S.; Raghavarao, K. S. Recent advances in nanoparticle based aptasensors for food contaminants. *Biosens. Bioelectron.* **2015**, *74*, 612–627.
- (12) Yuce, M.; Ullah, N.; Budak, H. Trends in aptamer selection methods and applications. *Analyst* **2015**, *140*, 5379–5399.
- (13) Silverman, S. K. Deoxyribozymes: DNA catalysts for bioorganic chemistry. *Org. Biomol. Chem.* **2004**, *2*, 2701–2706.
- (14) Silverman, S. K. In vitro selection, characterization, and application of deoxyribozymes that cleave RNA. *Nucleic Acids Res.* **2005**, *33*, 6151–6163.
- (15) Wang, Z.; Lee, J. H.; Lu, Y. Label-free colorimetric detection of lead ions with a nanomolar detection limit and tunable dynamic Range by using gold nanoparticles and DNAzyme. *Adv. Mater.* **2008**, *20*, 3263–3267.
- (16) Dalavoy, T. S.; Wernette, D. P.; Gong, M.; Sweedler, J. V.; Lu, Y.; Flachsbar, B. R.; Shannon, M. A.; Bohn, P. W.; Crokek, D. M. Immobilization of DNAzyme catalytic beacons on PMMA for Pb²⁺ detection. *Lab Chip* **2008**, *8*, 786–793.
- (17) Zhang, M.; Ge, L.; Ge, S.; Yan, M.; Yu, J.; Huang, J.; Liu, S. Three-dimensional paper-based electrochemiluminescence device for simultaneous detection of Pb²⁺ and Hg²⁺ based on potential-control technique. *Biosens. Bioelectron.* **2013**, *41*, 544–550.
- (18) Fu, L.; Zhuang, J.; Lai, W.; Que, X.; Lu, M.; Tang, D. Portable and quantitative monitoring of heavy metal ions using DNAzyme-capped mesoporous silica nanoparticles with a glucometer readout. *J. Mater. Chem. B* **2013**, *1*, 6123–6128.
- (19) Zhang, J.; Tang, Y.; Teng, L.; Lu, M.; Tang, D. Low-cost and highly efficient DNA biosensor for heavy metal ion using specific DNAzyme-modified microplate and portable glucometer-based detection mode. *Biosens. Bioelectron.* **2015**, *68*, 232–238.
- (20) Zhang, Y.; Xiao, S.; Li, H.; Liu, H.; Pang, P.; Wang, H.; Wu, Z.; Yang, W. A Pb²⁺-ion electrochemical biosensor based on single-stranded DNAzyme catalytic beacon. *Sens. Actuators, B* **2016**, *222*, 1083–1089.
- (21) Mazumdar, D.; Liu, J.; Lu, G.; Zhou, J.; Lu, Y. Easy-to-use dipstick tests for detection of lead in paints using non-cross-linked gold nanoparticle-DNAzyme conjugates. *Chem. Commun. (Cambridge, U. K.)* **2010**, *46*, 1416–1418.
- (22) Fan, C.; He, S.; Liu, G.; Wang, L.; Song, S. A portable and power-free microfluidic device for rapid and sensitive lead (Pb²⁺) detection. *Sensors* **2012**, *12*, 9467–9475.
- (23) Liu, X. L.; Wang, Y. Z.; Song, Y. J. Visually multiplexed quantitation of heavy metal ions in water using volumetric bar-chart chip. *Biosens. Bioelectron.* **2018**, *117*, 644–650.
- (24) Park, M.; Ha, H. D.; Kim, Y. T.; Jung, J. H.; Kim, S. H.; Kim, D. H.; Seo, T. S. Combination of a sample pretreatment microfluidic device with a photoluminescent graphene oxide quantum dot sensor for trace lead detection. *Anal. Chem.* **2015**, *87*, 10969–10975.
- (25) Zhao, L.; Wu, T.; Lefevre, J. P.; Leray, I.; Delaire, J. A. Fluorimetric lead detection in a microfluidic device. *Lab Chip* **2009**, *9*, 2818–2823.

NOTE ADDED AFTER ASAP PUBLICATION

This paper was originally published ASAP on December 12, 2019. The limit of detection was revised from 0.768 ppb to 0.44 ppb, and the corrected version was reposted on December 16, 2019.